

## AN END-TO-END TEST OF NEUTRON STARS AS PARTICLE ACCELERATORS

Patrizia A. Caraveo

INAF IASF-Milano, Via Bassini, 15; 20133 Milano; Italy

### ABSTRACT

Combining resolved spectroscopy with deep imaging, XMM-Newton is providing new insights on the particle acceleration processes long known to be at work in the magnetospheres of isolated neutron stars. According to a standard theoretical interpretation, in neutron stars' magnetospheres particles are accelerated along the B field lines and, depending on their charge, they can either move outward, to propagate in space, or be funnelled back, towards the star surface. While particles impinging on the neutron star surface should heat it at well defined spots, outgoing ones could radiate extended features in the neutron star surroundings.

By detecting hot spots, seen to come in and out of sight as the star rotates, as well as extended features trailing neutron stars as they move in the interstellar medium, XMM-Newton provides the first end-to-end test to the particle acceleration process.

Key words: Neutron stars; pulsars; Geminga; ESA; X-rays.

### 1. INTRODUCTION

Isolated neutron stars (INSs) are natural particle accelerators. Their, presumably dipolar, rapidly rotating magnetic fields, naturally inclined with respect to the star rotation axis, induce electric fields ideally suited to accelerate particles already present in the stars' magnetospheres or extracted from the crusts. Following the seminal paper of Goldreich and Julian (1969) and Sturrock (1971), a lot has been done to work out the details of such an acceleration, focusing on its most likely location(s) inside the INS magnetosphere and on its efficiency. Traditionally, two classes of models have been developed: on one side the polar cap ones (Ruderman & Sutherland, 1975, Harding & Daugherty, 1998, Rudak & Dyck, 1999), where the acceleration takes place near the star surface, just above the magnetic pole; on the other side, the outer gap ones (Romani, 1996), where the acceleration is taking place in the outer magnetosphere, not far from the light cylinder. Recently, the slot gap model, extending

from the polar cap to the light cylinder, has been added as a third alternative (Muslinov & Harding, 2003, Dyck & Rudak, 2003, Harding, 2005). Notwithstanding important differences between models, the interaction between accelerated particles (typically electrons) and the star magnetic field results in the production of high energy gamma-rays which, in turn, are not able to escape the highly magnetic environment and are converted into electron positron pairs. This initiates a cascade rapidly filling the magnetosphere with energetic particles which, interacting with the magnetic field, are responsible for the vast majority of the INSs' multiwavelength phenomenology.

### 2. ACCELERATION BY-PRODUCTS

INSs are mainly studied through their non thermal radio emission. Radio searches have been highly successful and the current radio catalogues list more than 1500 pulsars (Manchester et al. 2005).

In spite of the sheer number of objects and their very diverse phenomenology, INS radio emission accounts for a negligible fraction of the star rotational energy loss. A far more important fraction of the star energy reservoir goes into high-energy radiation, mainly in high-energy gamma-rays. While the number of objects shrinks to less than 1% of the radio ones (Thompson et al., 2001), in gamma rays the INSs' luminosity can reach a sizable fraction of the total rotational energy loss, with an increase in efficiency for the older objects.

The rich INSs' phenomenology encompasses now also X and optical emissions. While the numbers are slightly higher than the gamma-ray ones (a dozen in the optical (Caraveo, 2000, Mignani et al. 2004) and two scores in X-rays (Becker & Aschenbach, 2002) the nature of the radiation is not as clear cut as in the radio or gamma-ray domains. In the optical, as well as in X-rays, aged neutron stars exhibit both thermal and non-thermal emissions. Indeed, when non-thermal emission somewhat weakens with age, the thermal one begins to emerge to tell the story of the cooling crust of the neutron star. INS thermal emission, however, is not totally unrelated to the magnetospheric particle acceleration. Depending

on their electric charge, particles move in different directions along the magnetic field lines. While those moving outward try to escape the INS magnetosphere, those moving inward hit the star and heat its crust at well defined spots, that, under the assumption of a dipolar magnetic field, should coincide with its polar caps (return currents, see e.g. Ruderman & Sutherland 1975; Arons & Scharlemann 1979). Thus, thermal emission could be of use to trace non-thermal phenomena.

The escaping particles, on the other side, are part of the neutron stars' relativistic wind which is supposed to account for the bulk of their observed rotational energy loss. Such relativistic wind can be traced through its interaction with the interstellar medium (ISM), both in the immediate surroundings of the stars, where the INS magnetic field is still important, or farther away, where the wind radiation pressure is counterbalanced by the shocked ISM. An important player to determine the shape and the phenomenology of the resulting Pulsar Wind Nebula (PWN) is the actual neutron star speed. INSs are known to be high velocity objects and, plunging supersonically through the ISM, they can give rise to a rich bow shocks phenomenology seen in the radio, optical and X-ray domains (e.g. Chattarjee & Cordes, 2002).

Fig.1 summarizes the neutron star *acceleration tree*: starting from the synoptic view (Harding, 2005) of the mechanisms responsible the gamma ray emission (the aspect most intimately related to the actual particle acceleration) and following the destiny of the particle moving inward (left) and outward (right). Using past and present space observatories operating at X and gamma-ray domain, we can construct such a tree with the aim to improve our understanding of the neutron star physics.

### 3. THE OBSERVATIONAL PANORAMA

Our task is now to briefly review the data related to the three steps highlighted in Fig.1 in order to find INSs observed throughout the *acceleration tree*.

#### 3.1. High-energy gamma-rays

Waiting for the next generation of gamma-ray instruments such as Agile (Tavani et al., 2003) and Glast (Michelson et al., 2003), we try to make the best use of the EGRET results. INSs (be they radio loud or radio quiet) are the only class of galactic sources firmly identified as high-energy gamma-rays emitters. Indeed, pulsars are especially appealing to gamma-ray astronomers since their timing signature allows to overcome the identification problem due to the relatively large gamma-ray error boxes. However, in spite of more than a decade of relentless efforts based on the EGRET data, only Crab, Vela, PSR 1706-44, PSR1951+32, PSR1055-52 and the radio quiet Geminga are confirmed gamma-ray sources (Thompson et al., 2001). A few more pulsars have been

proposed as sources of pulsed gamma-radiation, but the claims are still awaiting confirmations. Several positional coincidences between newly discovered pulsars and old Egret sources (Hartman et al. 1999) have been reported, but, again, such suggestions cannot be confirmed without an operating gamma-ray telescope. Thus, for the moment being, our gamma-ray sample encompasses a very young (and energetic) object such as the Crab, two slightly older pulsars (Vela, PSR 1706-44) and three middle-aged INSs (PSR1055-57, Geminga and the fast spinning PSR1951+32). It is worth noting that the efficiency for conversion of rotational energy loss into gamma-rays changes as a function of pulsar age. It goes from the value of  $\sim 0.009\%$ , for the Crab, to several %, for Geminga and PSR 1055-57.

#### 3.2. Hot spots

The presence of hot spots on the surface of INSs has been long suspected on the basis of their overall X-ray spectral shape requiring more than a simple black-body to describe the data. Usually two black-body curves, characterized by different temperatures and emitting areas, are needed to fit the X-ray spectra for all but the very youngest INSs. A slightly colder black-body, covering the majority of the INS surface, provides the bulk of the X-ray luminosity while a hotter one, covering a smaller surface, is needed to obtain a satisfactory spectral fit.

Long XMM-Newton observations of Geminga, PSR0656+14 and PSR 1055-57, three middle-aged, rather similar INSs, have added an important piece of information. Taking advantage of their exceptional photon harvest, De Luca et al (2005a) were able to perform space resolved spectroscopy of the three INSs. For all objects they have shown that

- the spectra are varying significantly throughout the rotational phase
- the hot blackbody contribution is the most dramatically variable spectral component.

This is shown in Fig.2 where the emitting radii, computed on the basis of the phase-resolved spectral fits, are shown as a function of the pulsar rotational phase. While for PSR B0656+14 the modulation in the emitting radius wrt. the average value is  $<10\%$ , similar to the value found for the cool blackbody component, in the case of PSR B1055-52 we see a 100% modulation, since the hot blackbody component is not seen in 4 out of 10 phase intervals. A similar, 100% modulation is observed also for Geminga, although in this case the hot blackbody component is seen to disappear in just one phase interval, and the profile of its phase evolution is markedly broader. It is natural to interpret such marked variations as an effect of the star rotation, which alternatively brings into view or hides one or more hot spots on the star surface. As outlined above, such hot spots arise when charged particles, accelerated in the magnetosphere, fall back to the polar caps along magnetic field lines. Straight estimates of neutron star polar cap sizes, based on a simple "centered" dipole magnetic field geometry (polar

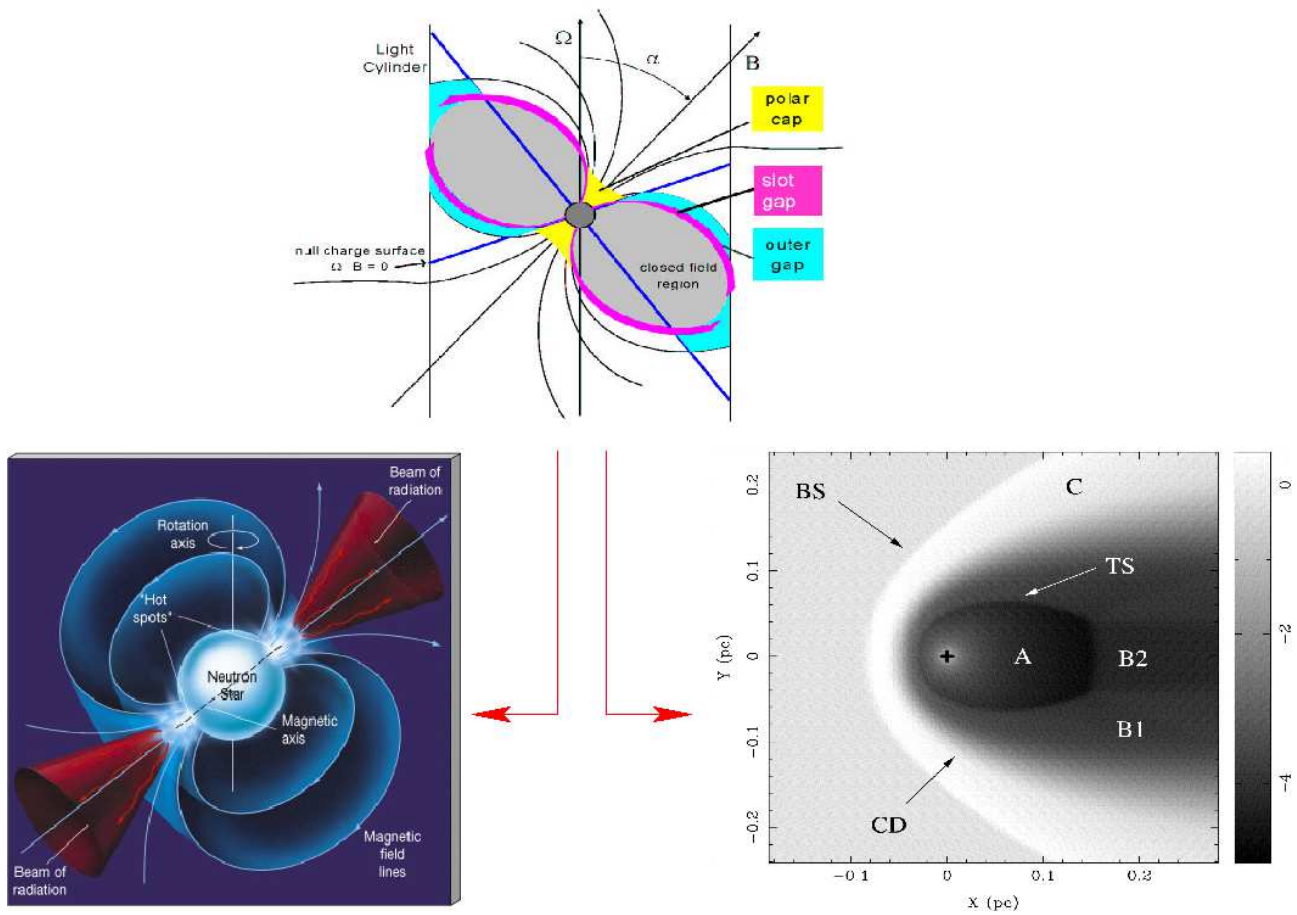


Figure 1. Neutron star acceleration tree. Top panel : schematic view of a pulsar magnetosphere showing the gamma-ray emitting regions, according to the various classes of models (from Harding, 2005). Bottom left: a similar view of a pulsar magnetosphere showing the hot spots on the pulsar polar caps. Bottom right: hydrodynamic simulation of a bow shock (BS) generated by the interaction of the isotropic relativist wind of a neutron star (marked with a cross), moving horizontally from right to left, with the ISM (Gaensler et al, 2004). A indicates the pulsar wind cavity, where the electrons propagate freely, B is used for the shocked pulsar wind material, while C represents the shocked ISM. The termination shock, TS, is where the energy density of the pulsar wind is balanced by the external pressure, while CD is the contact discontinuity bounding the shocked pulsar wind material.

cap radius  $R_{PC} = R\sqrt{\frac{R\Omega}{c}}$ , where  $R$  is the neutron star radius,  $\Omega$  is the angular frequency and  $c$  is the speed of light), predict very similar radii for the three neutron stars, characterized by similar periods (233 m for PSR B0656+14, 326 m for PSR B1055-52 and 297 m for Geminga, assuming a standard neutron star radius of 10 km). The observed radii are instead markedly different, with values ranging from  $\sim 60$  m for Geminga to  $\sim 2$  km for PSR B0656+14 (see De Luca et al, 2005a for a detailed discussion).

While waiting to enlarge the sample of deeply scrutinized X-ray pulsars, it does not come as a surprise that two of the three objects showing direct evidence for the presence of rotating hot spots are highly efficient gamma-ray sources.

### 3.3. Pulsar Wind Nebulae

When the particle wind from a fast moving INS interacts with the surrounding ISM, it gives rise to complex structures, globally named ‘‘Pulsar Wind Nebulae’’ (PWNe) where  $\sim 10^{-5} - 10^{-3}$  of the NS  $\dot{E}_{rot}$  is converted into electromagnetic radiation (for recent reviews see Gaensler et al 2004, and Gaensler 2005). The study of PWNe may therefore give insights into aspects of the neutron star physics which would be otherwise very difficult to access, such as the geometry and energetics of the particle wind and, ultimately, the configuration of the INS magnetosphere and the mechanisms of particle acceleration. Moreover, PWNe may probe the surrounding medium, allowing one to measure its density and its ionisation state.

A basic classification of PWNe rests on the nature of the external pressure confining the neutron star wind (e.g. Pellizzoni et al. 2005). For young NSs ( $< \text{few } 10^4$  y) the pressure of the surrounding supernova ejecta is effective and a ‘‘static PWN’’ is formed. For older systems ( $> 10^5$  y) the neutron star, after escaping the eventually faded supernova remnant, moves through the unperturbed ISM and the wind is confined by ram pressure to form a ‘‘Bow-shock’’ PWN.

Static PWNe (Slane, 2005, for a review) usually show complex morphologies. Striking features such as tori and/or jets (as in the Crab and Vela cases), typically seen in X-rays, reflect anisotropies of the particle wind emitted by the energetic, central INS and provide important constraints on the geometry of the system. A remarkable axial symmetry, observed in several cases, is assumed to trace the rotational axis of the central INS. For the Crab and Vela PWNe, such an axis of symmetry was found to be coincident with the accurately measured direction of the INS proper motion (Caraveo & Mignani 1999, Caraveo et al. 2001). This provided evidence for an alignment between the rotational axis and the proper motion of the two neutron stars, with possible important implications for the understanding of supernova explosion mechanisms (Lai et al. 2001). The alignment between spin axis and space

velocity, directly observed only for Crab and Vela, is now assumed as a standard property of NSs (Ng & Roman, 2004).

Bow-shocks (for a review see Pellizzoni et al. 2005, Gaensler et al 2004) have a remarkably simpler, ‘‘velocity-driven’’ morphology. They are seen frequently in  $H_\alpha$  as arc-shaped structures tracing the forward shock, where the neutral ISM is suddenly excited. In other cases, X-ray emission (and/or radio emission on larger scales) is seen, with a cometary shape elongated behind the neutron star, due to synchrotron radiation from the shocked NS particles downstream (only in the case of PSR B1957+20 both the  $H_\alpha$  and the X-ray structures have been observed, Stappers et al., 2003). According to the lower energetics of the central, older INS, bow shocks are typically fainter than static PWNe and proximity is a key parameter for their observation.

Since we aim at tracing the high energy particle escaping the INS magnetosphere, we concentrate on the X-ray PWNe. Inspecting the list of Gaensler et al (2004), we find only PSR B1951+32 in common with the gamma-ray database, leaving little hope to find an object displaying all the aspects of the *acceleration tree*.

However, recent observations of Geminga, combined with previous ones by XMM-Newton, have unveiled the presence of a bona fide PWN with complex diffuse features trailing the pulsar perfectly aligned with its well known proper motion (De Luca et al., 2005b; Caraveo et al. 2003).

Thus, the combined EGRET, XMM-Newton and Chandra results on Geminga make this source the most suitable example for our end-to-end test of particle acceleration. For a review on the multiwavelength phenomenology of Geminga, see Bignami & Caraveo (1996).

## 4. GEMINGA AS A TEST CASE

Fig.3 summarizes all the observational evidence collected so far on the presence of high energy electrons/positrons in the magnetosphere of Geminga. First, the EGRET light-curve whose  $> 100$  MeV photons could not have been produced without high energy particles and magnetic fields.

Next, the contribution of a 100 ksec XMM-Newton observation which yielded both

a) the evidence for the presence of minute hot spot(s) varying throughout the pulsar phase (Caraveo et al., 2004)

b) the detection of two elongated tails, trailing the pulsar in its supersonic motion through the ISM and perfectly aligned with the proper motion direction. The flat spectral shape of the tails’ X-ray photons suggests a synchrotron origin which, combined with the typical magnetic field present in a shocked ISM, implies the presence of  $\sim 10^{14}$  eV electrons/positrons, i.e. of particle at the upper limit of the energy range achievable for an INS like Geminga. Moreover, the lifetime of such electrons (or, more precisely, the time it takes for them to lose half of their en-

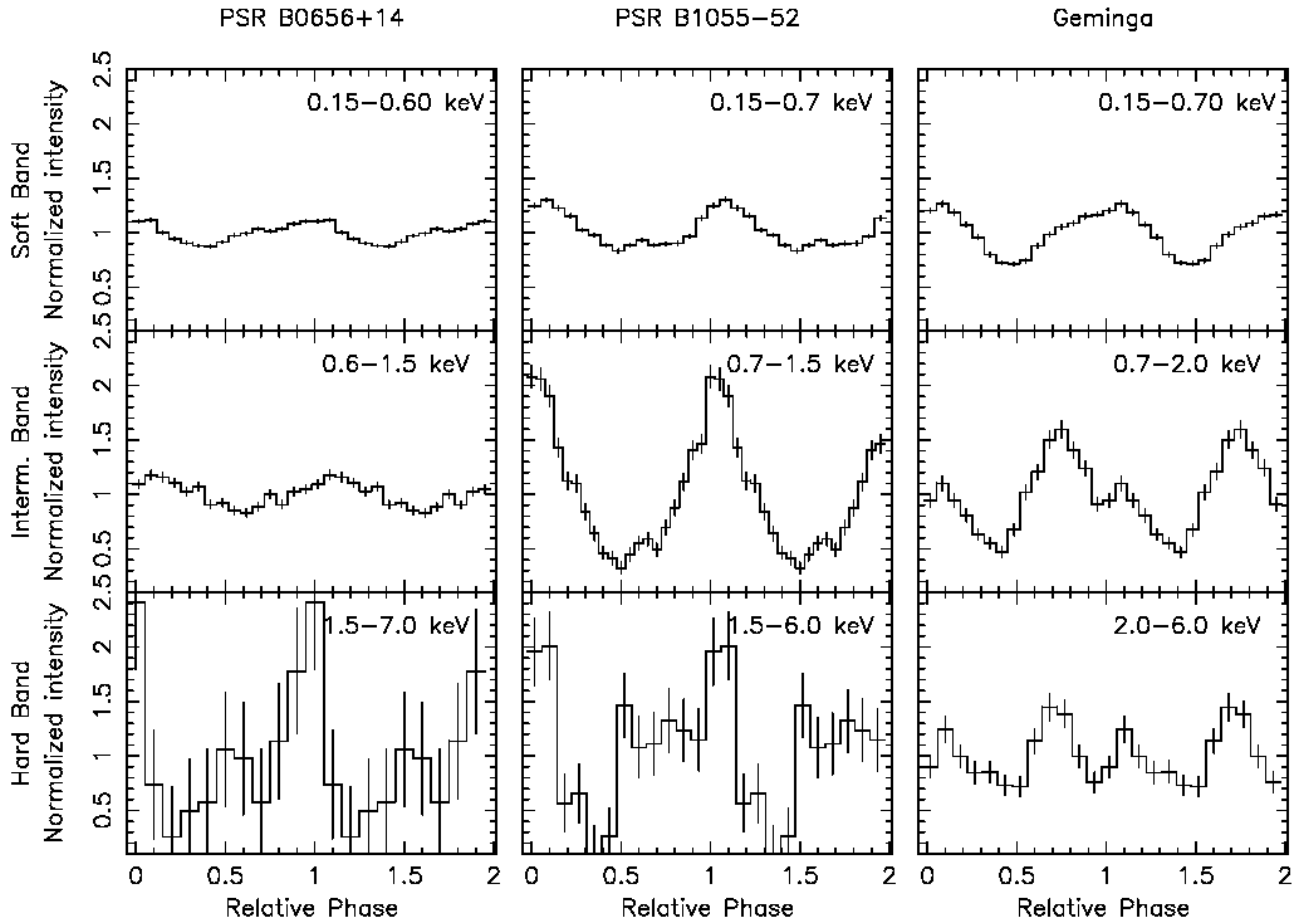


Figure 2. Energy-resolved light curves of PSR B0656+14, PSR B1055-52 and Geminga in different energy ranges. To ease the comparison of the behaviour of the three INSs, all light curves have been plotted setting phase 0 to the X-ray maximum. Pulsed fractions (computed as the ratio between the counts above the minimum and the total number of counts) are as follows: PSR B0656+14  $12.3 \pm 0.4\%$  in 0.15-0.6 keV,  $16.9 \pm 2.3\%$  in 0.6-1.5 keV,  $75 \pm 20\%$  in 1.5-7.0 keV; PSR B1055-52  $16.7 \pm 0.6\%$  in 0.15-0.7 keV,  $67 \pm 3\%$  in 0.7-1.5 keV,  $90 \pm 10\%$  in 1.5-6.0 keV; Geminga  $28.4 \pm 0.6\%$  in 0.15-0.7 keV,  $54.5 \pm 2.4\%$  in 0.7-2.0 keV,  $33 \pm 5\%$  in 2.0-6.0 keV.

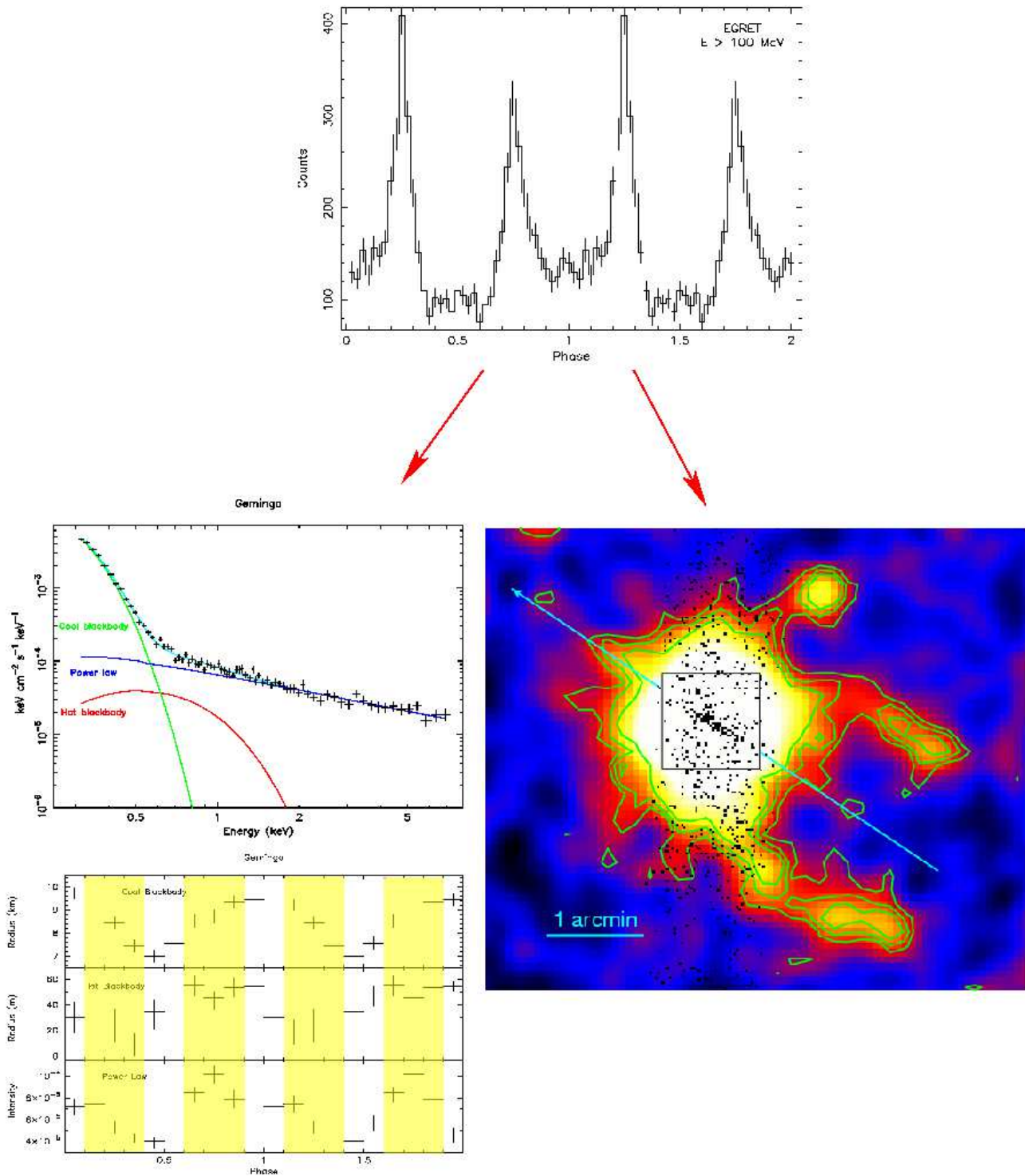


Figure 3. The acceleration tree as observed for Geminga. Top: the gamma-ray light curve. Left: the XMM-Newton average spectrum as well as the results of phase-resolved spectroscopy, showing the evolution of the black-body emitting regions as a function of the INS rotational phase. The shaded area mark the phase intervals corresponding to the  $\gamma$ -ray peaks observed by EGRET. The highest  $\gamma$ -ray peak occurs at phase  $0.25 \pm 0.15$ , the second one at phase  $0.75 \pm 0.15$  (the uncertainty is due to the extrapolation of the EGRET ephemeris to the epoch of the XMM-Newton observation). Right: Geminga as seen by Chandra and XMM-Newton (from De Luca et al., 2005b). The Chandra image, rebinned to a pixel size of  $2''$  has been superposed on the XMM-Newton/MOS image obtained by Caraveo et al.(2003). Surface brightness contours for the XMM image have been also plotted. The ACIS field of view is limited to a rectangular region 1 arcmin wide. The pulsar proper motion direction is marked by an arrow.

ergy) in the bow-shock magnetic field is  $\sim 800$  years. On the other hand, Geminga's proper motion (170 mas/year) allows one to compute the time taken by the pulsar and its bow shock to transit over the apparent length of the x-ray structures in the sky ( $3'$  from the central source). Such a time is close to 1,000 years. Thus, Geminga's tails remain visible for a time comparable to the electron synchrotron X-ray emission life time after the pulsar passage. The comet-like structure seen by Chandra is as luminous as the larger and fainter tails and its spectrum is equally hard.

Hot spot(s), elongated, faint tails and short, brighter trail have roughly the same luminosity, corresponding to  $\sim 10^{-6}$  of its  $\dot{E}_{rot}$ .

We note that the morphology and hard spectrum of the Trail is reminiscent of the jet-like collimated outflows structures seen in the cases of Crab and Vela (Helfand et al., 2001, Pavlov et al. 2003, Willingale et al., 2001, Mori et al. 2004) and associated to the neutron stars spin axis direction. In particular, the small Geminga's Trail can be compared to the "inner counterjet" of the Vela PSR (Pavlov et al., 2003), characterized by a similar spectrum (photon index  $\sim 1.2$ ) and efficiency ( $L_X \sim 10^{-6} \dot{E}$ ). The projected angle between Geminga proper motion and its backward jet is virtually null, which implies that also the pulsar spin axis should be nearly aligned with them. Geminga would thus be the third observed neutron star having its rotational axis aligned with its space velocity, after the cases of the Crab and Vela.

The whole scenario, encompassing both the large Tails and the small Trail, could therefore fit in the frame of an anisotropic wind geometry. It includes jet structures along the spin axis and relativistic shocks in the direction of the magnetic axis where most of the wind pressure is concentrated due to the near radial outflow from magnetosphere open zones.

The coupling of the jet-like Trail seen by Chandra with the larger, arc-shaped Tails seen by XMM has no similarity with other pulsars.

## 5. CONCLUSION

The particle acceleration going on in an INS magnetosphere can now be traced from end-to-end. While gamma ray emission probes directly the particle population in the magnetosphere, using the current generation of X-ray observatories we are now able to follow the destiny of the particles traveling up and down the magnetic field lines through the study of hot spots on the star surface and of PWNe. The same process responsible for the copious gamma-ray emission of Geminga would thus also be responsible for the appearance of the hot spots on its surface (Halpern & Ruderman, 1993). Such a strong link between the X-and gamma-ray behaviour of the source could be exploited to map the relative positions of the regions responsible for the different emissions. A precise comparison of the source X and gamma-ray light curves

is crucial at this point, but the lack of operating high energy gamma ray telescope makes it impossible. Simultaneous observations performed by XMM-Newton and by Agile and/or GLAST (foreseen to be operational in the coming years) will add important pieces of information to test INSS' capability to accelerate particles.

## ACKNOWLEDGMENTS

This analysis of XMM-Newton as well as Chandra data is supported by the Italian Space Agency (ASI).

## REFERENCES

- [1] Arons, J. & Scharlemann, E.T., 1979, ApJ 231, 854
- [2] Becker, W.; Aschenbach, B., 2002, MPE Report 278. Edited by W. Becker, H. Lesch, and J. Trmper. Garching bei Mnchen: Max-Planck-Institut fr extraterrestrische Physik, 64
- [3] Bignami, G.F. & Caraveo, P.A. 1996, Ann.Rev. Astron. Astrophys. 34,331
- [4] Caraveo, P.A. 2000 in "Pulsar Astronomy - 2000 and Beyond", ASP Conference Series, Ed.s M. Kramer, N. Wex, and N. Wielebinski, 202,289
- [5] Caraveo, P.A., De Luca, A., Mereghetti, S., Pellizzoni, A., Bignami, G.F., 2004, Science 305, 376
- [6] Caraveo, P.A., Bignami, G.F., De Luca, A., et al., 2003, Science 301, 1345
- [7] Caraveo, P.A., De Luca, A., Mignani, R.P., Bignami, G.F., 2001, ApJ 561, 930
- [8] Caraveo, P.A., Mignani, R.P., 1999, A&A 344, 367
- [9] Chatterjee, S. & Cordes, J. M., 2002, Ap.J. 575, 407
- [10] De Luca, A. et al. 2005a Ap.J, 623, 1051
- [11] De Luca, A. et al. 2005b A&A in press (astro-ph/0511185)
- [12] Dyks, J. and B. Rudak, 2003, Ap.J., 598, 1201
- [13] Gaensler, B.M., van der Swaluw, E., Camilo, F., et al., 2004, ApJ 616, 383
- [14] Gaensler, B.M., 2005, "Young Neutron Stars and Their Environment", ASP Conf.Proc., eds F.Camilo and B.M.Gaensler, p.151 7)
- [15] Goldreich, P. Julian, W.H., 1969, Ap.J.,157, 869
- [16] Halpern J.P. and M. Ruderman, 1993, Ap.J., 415,286
- [17] Harding, A. K. and J. K. Daugherty, 1998, Adv. Space Res. 21, 251
- [18] Harding, A. K. 2005, Proceedings of the 22nd Texas Symposium on Relativistic Astrophysics at Stanford University, Stanford, 2004, edited by P. Chen et al., eConf C041213
- [19] Hartman, R.C. et al., 1999, Ap.J.S.,123,79
- [20] Helfand, D.J., Gotthelf, E.V., Halpern, J.P., 2001, ApJ 556, 380
- [21] Lai, D., Chernoff, D.F., Cordes, J.M., 2001, ApJ 549, 1111

- [22] Manchester, R.N. et al., 2005, *A.J.*, 129, 1993
- [23] P.F. Michelson *SPIE*, 2003, 4851, 1144  
<http://www-glast.stanford.edu/>
- [24] Mignani, R. P., de Luca, A., Caraveo, P. A., 2004, *IAU Symposium no. 218* Ed.s Fernando Camilo and Bryan M. Gaensler. *Astronomical Society of the Pacific*, 2004, 391
- [25] Mori et al., 2004, *ApJ*, 609, 186
- [26] Muslimov, A. G. and A. K. Harding, 2003, *Ap. J* 588, 430
- [27] Ng, C.-Y., Romani, R.W., 2004, *ApJ* 601, 479
- [28] Pavlov, G.G., Teter, M.A., Kargaltsev, O., Sanwal, D., 2003, *ApJ* 591, 1157
- [29] Pellizzoni, A., Mattana, F., De Luca, A., et al., 2005, "High Energy Gamma-Ray Astronomy", eds. F.A. Aharonian, H.J.Vlk, D.Horns, *AIP Conference Proceedings*, 745, p.371
- [30] Romani, R. W., 1996, *Ap. J* 470, 469
- [31] Rudak, B. and J. Dyks, 1999, *Mon. Not. R. Astron. Soc.* 303, 477.
- [32] Ruderman, M. A. & P. G. Sutherland 1975 *Ap. J* 196, 51
- [33] Slane, P., 2005, *Adv.Sp.Res.* 35, 1092
- [34] Stappers, B.W., Gaensler, B.M., Kaspi, V.M., van der Klis, M., Lewin, W.H.G., 2003, *Science* 299, 1372
- [35] Sturrock, P. A., 1971 *Ap. J* 164, 529
- [36] Tavani, M. et al., 2003, *SPIE*, 4851, 1151  
<http://agile.mi.iasf.cnr.it>
- [37] Thompson, D. J., 2001 in *High Energy Gamma-Ray Astronomy*, eds. F. A. Aharonian, H. Volk, *AIP Conf. Proc.* 558, p. 103112, 2001.
- [38] Zhang, B. and A. K. Harding, 2000, *Ap. J* 532, 1150
- [39] Willingale et al., 2001, *A&A*, 365, L212